Thermal Recovery of Bitumen From the Grosmont Carbonate Formation—Part 1: The Saleski Pilot

Moslem Hosseininejad Mohebati and **Daniel Yang,** Laricina Energy Limited, and
Jeff MacDonald, Osum Oil Sands Corporation*

Summary

The Grosmont formation, a carbonate reservoir in Alberta, Canada, has 400 billion bbl of bitumen resource, which is currently not commercially exploited. The carbonate reservoir is karstified by groundwater and tectonically fractured, resulting in three classes of porosity: matrix, vugs, and fractures. The viscosity of bitumen is lowered by four to six orders of magnitude when heated by steam.

Since December 2010, the Saleski pilot project evaluated steam-injection-recovery processes by use of four well pairs, two each in the Grosmont C and Grosmont D units. For the first year of the pilot, two well pairs were operated with continuous injection and production similar to successful steam-assisted-gravity-drainage (SAGD) projects in Alberta oil sands. Reservoir observations of steam/oil ratio (SOR) and calendar-day oil rate (CDOR) indicate recovery by gravity drainage is viable, although operating practices from conventional SAGD must be modified for the Grosmont formation.

The decision to evaluate cyclic injection and production from single wells was made in early 2012, although it was recognized that cyclic operations created new challenges for the facility (which was built for SAGD operations) and artificial lift. The pilot data indicate that the drilling conditions (balanced vs. overbalanced), completions (openhole vs. slotted liner), and acid treatments of the wells have a significant impact on the individual-well performance.

Injectivity into the Grosmont reservoir is high, even into a cold reservoir, because of the existing fracture system. Injection pressures stayed less than 40% of the estimated pore pressure required to lift the overburden. 4D-seismic results indicate that the injection conformance along the well axis is close to 100% and that the heated area is laterally contained around the well.

Productivity is comparable to oil-sands project performance. The decline of oil rate is not only dependent on pressure but also on temperature. For cyclic operations, a CDOR of 43 m^3/d (for a 450-m-long well) and an SOR of 3.4 were achieved, demonstrating that with sufficient scale, a commercial project can be established successfully.

The pilot has satisfactorily derisked the Grosmont reservoir at Saleski. While cyclic operations have demonstrated economic performance, continuous injection and production similar to SAGD remains an alternative recovery strategy beyond startup in the later depletion stage. Successful future developments will advance the optimization of drilling, completion, artificial-lift, and plant-capacity issues, while the reservoir itself has demonstrated its production capacity.

Introduction

Of the estimated 1.8 trillion bbl of bitumen resource in Alberta, approximately 30% is located in carbonate rocks, with 400 billion bbl in the Grosmont formation (Burrowes et al. 2011). On the basis of the ultrahigh viscosity of bitumen (up to tens of millions of cp at reservoir conditions) and the uncertainty of flow performance in naturally fractured reservoirs when applying a recovery process that involves injection, this vast resource is currently not exploited.

In December 2010, following a hiatus of approximately 25 years, a joint venture between Laricina Energy Limited and Osum Oil Sands Limited established a proprietary Grosmont steam-injection pilot in the Saleski field, to which the pilot performance data become publicly available in 2014. This paper provides an overview of the large volume of information and a context of the conditions under which it was achieved. Data discussed here end 31 August 2013.

The first attempts to produce bitumen from the Grosmont formation date back to the mid-1970s and continued through the 1980s when Chevron, Unocal Corporation, Alberta Oil Sands Technology and Research Authority, and Canadian Superior operated steam-stimulation and combustion pilots (for an overview of Grosmont pilots, see **Table 1;** McDougall et al. 2008; Yuan et al. 2010). A discussion of the early Saleski pilot is found in Solanki et al. (2011).

Pilot data are presented and analysed in this paper (Part 1), and form the basis for interpretation and forward planning in Part 2 (Yang et al. 2014). The paper starts by describing the Saleski pilot location, reservoir geology, wells, and facility, and presents a high-level overview of the operational history. The discussion then focusses on a subsection of the reservoir, with separate analyses of continuous and cyclic steam injection. Injectivity and productivity of the wells are discussed and compared.

It is not possible to discuss all information from the Saleski pilot in a single publication. Details from tracer and solvent-injection tests, bitumen "finger printing" analysis, and well stimulation with acid, as examples, will be published in separate papers; however, the results from these additional studies contributed to the overall interpretation discussed here.

The Saleski Pilot

Fig. 1 shows the location of the Saleski pilot. The project site is approximately 350 km north of Edmonton, Alberta. It is located in the Grosmont formation trend with a net pay thickness of more than 40 m.

Geology. The Grosmont formation was deposited in a shallow marine tropical sea approximately 380 million years ago (Ma) during the Upper Devonian period. It subsequently underwent subsidence and greater than 1000 m of burial during which the Grosmont formation was altered from limestone to dolomite. During the formation of the ancestral Rocky Mountains approximately (Laramide 100–60 Ma, Columbia 200–145 Ma), uplift of the western Canadian sedimentary basin commenced and the Grosmont formation underwent tectonic fracturing in a northeast/southwest direction because of torsional failure in the Proterozoic; a second set is oriented northwest/southeast. At approximately 120 Ma, the Grosmont formation underwent one phase of erosion and exposure to fresh meteoric water, resulting in karstification. At this time, the Grosmont dolomite underwent a period of intense leaching, resulting in the development of most of the porosity and permeability present in the Grosmont formation today. At approximately 118 Ma, the Grosmont formation underwent further subsidence and was buried by Cretaceous sediments of the Clearwater formation. The Grosmont formation was uplifted again

*Now with TransGlobe Energy Corporation.

Original SPE manuscript received for review 8 August 2013. Revised manuscript received for review 4 April 2014. Paper (SPE 171560) peer approved 16 June 2014.

TABLE 1—SUMMARY OF GROSMONT CARBONATE PILOTS (HUSKY OIL OPERATIONS 2013)

	Start	End	Comments
Chipewyan River			
Injectivity	Dec 1974	Apr 1975	Injectivity below fracture pressure
Buffalo Creek			
Single well CSS	Feb 1977	May 1977	One cycle
Single well CSS	Apr 1980	Jan 1987	12 cycles
Single well CSS	Sep 1983	Oct 1984	Three cycles
Single well CSS	Apr 1986	Nov 1986	Three cycles
Steam flood	May 1977	Oct 1977	Water channeling
Combustion	Jul 1978	Feb 1980	No success
McLean Creek			
Multi well CSS	Sep 1982	Oct 1984	Five-spot, 6 and 11 acres
Single well CSS	Nov 1984	Apr 1984	Eight cycles
Orchid			
Single well CSS	Apr 1985	Apr 1986	Three cycles
Saleski			
Single well CSS	May 1986	May 1987	Three cycles
Laricina			
Cold solvent	Oct 2008	Feb 2009	High injectivity, cold production
Continuous	Jan 2011	Feb 2012	Four well pairs
Cyclic	Mar 2012	Ongoing	Three to Five cycles
Sunshine			
Single well CSS	Jan 2011	Mar 2011	One cycle

CSS = cyclic steam stimulation.

approximately 60 Ma during the formation of the present day Rocky Mountains, followed by migration of oil into the Grosmont formation approximately 50 Ma. This light oil was biodegraded into bitumen by bacteria that were present in the associated formation water. Today at Saleski, the Grosmont bitumen reservoir is at a depth of approximately 350 m, or 230 m above sea level (Barrett and Hopkins 2010).

The Grosmont formation is subdivided into four units: A, B, C, and D, with the D-unit on top and being the youngest **(Fig. 2).** At Saleski, bitumen is confined to the two uppermost units: Grosmont C and D. The Grosmont C is approximately 33 m thick where it has not been subjected to erosion. It has been subdivided into three subunits: the Lower Argillaceous dolomite and the middle and upper Grosmont C, which are approximately 13, 13, and 7

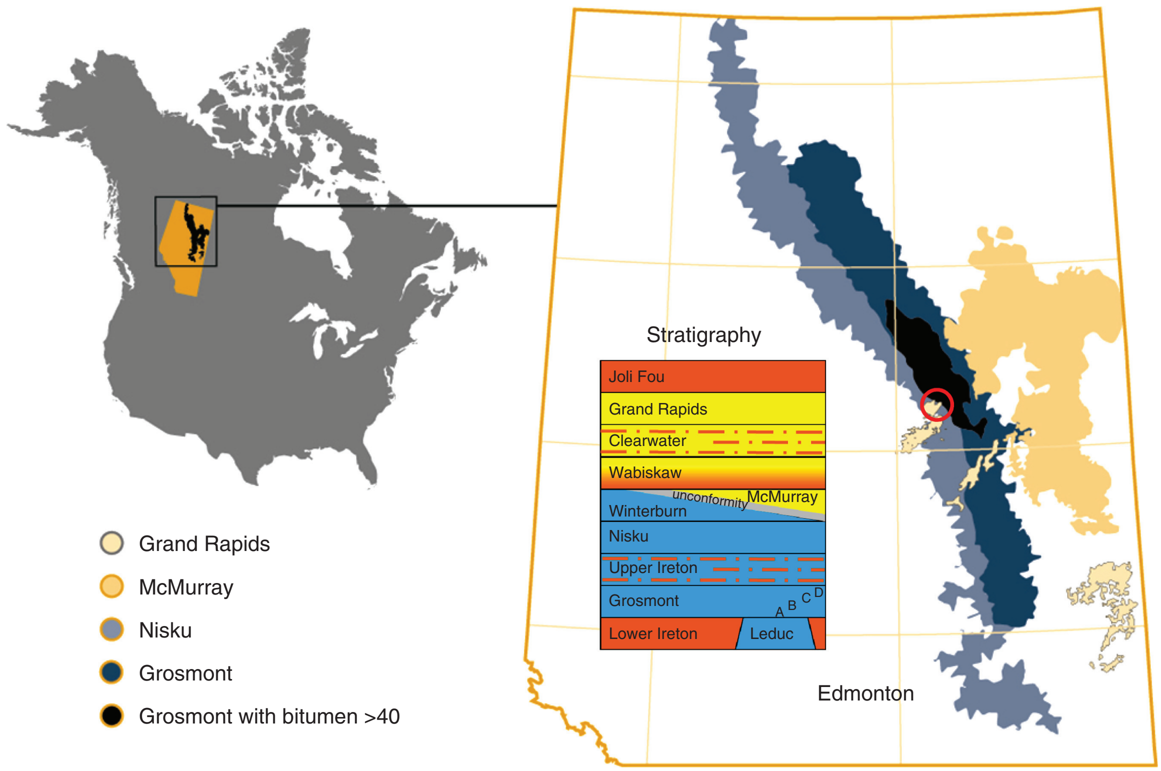

Fig. 1—Location of Saleski pilot (red circle), together with bitumen-bearing formations and major stratigraphic units (brown = shale, yellow = sand, and blue = dolomite and limestone).

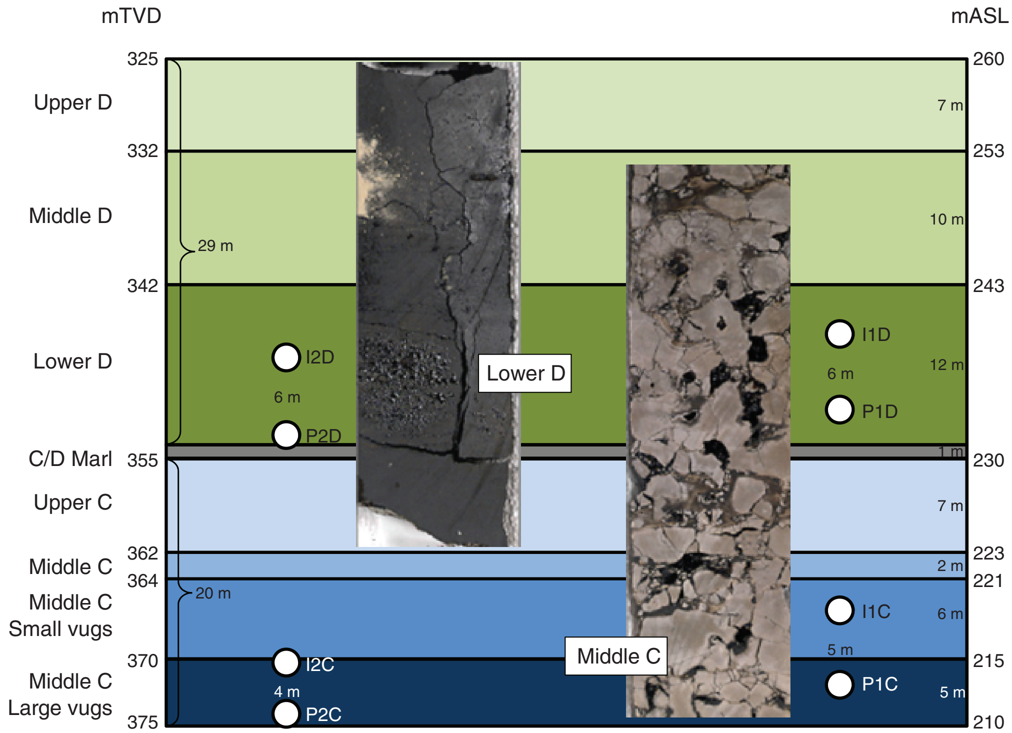

Fig. 2—Grosmont C and D reservoir subunits in a cross section with approximate horizontal-well position. Core photos are discussed in the text. The width of a core photo is 7 to 8 cm.

m thick, respectively. The Grosmont C Lower Argillaceous dolomite unit is a shaley dolomite and is considered nonreservoir. The Grosmont C middle unit is a dolomite that can be further subdivided into three subunits: large vugs, small vugs, and disaggregated dolomite, from bottom to top. The lowest subunit has abundant vugs greater than 0.5 cm in diameter that are a product of leaching of fossil burrows. Intervals between vugs are commonly connected by cracks, which are typically less than 3 cm long, subvertical, and lacking in a preferred direction. The small-vug unit is a stromatoporoid-rich interval, dominated by 0.1- to 0.5-cm-diameter vugs formed by leaching of fossil material. This interval is less fractured than the underlying subunit. The disaggregated-dolomite interval is 2 m thick and grades between a laminated dolomite with significant fine-pore matrix porosity and bitumen-saturated dolomite consisting of silt-sized dolomite crystals. The more consolidated portion of this interval is moderately to highly fractured. The upper Grosmont C unit is a clean, very-fine- to fine-grained, laminated dolomite grainstone. This is a small-vug (vugs less than 0.5 cm in diameter) reservoir facies, which has good intraparticle and intercrystalline porosity.

The Grosmont C/D marl separates the Grosmont C and D units. It consists of a 1-m-thick white dolo-mudstone with irregular wisps of shale that is capped by a 0.5- to 1.0-m-thick interlaminated siliciclastic green shale and fine bitumen-saturated disaggregated-dolomite interval. The laminated green shale is lithologically similar to the green-shale interval that caps the middle Grosmont D subunit.

The Grosmont D unit is approximately 30 m thick and has been divided into three subdivisions: the lower, middle, and upper units, which are approximately 12, 10, and 8 m thick, respectively. The lower Grosmont D subunit is a bitumen-saturated, porous interval. At Saleski, it is mainly a karst breccia composed of angular clasts of white dolomite encased in a matrix of bitumen-saturated fine disaggregated dolomite crystals. The porosity type is mainly interparticle within the matrix. The middle Grosmont D subunit has a mixed lithology consisting of wispy/laminated dolomudstone overlain by amphipora-floatstone, and capped by a thin unit consisting of green siliciclastic shale interlaminated with dolomite mudstone. The middle Grosmont D subunit has a moderate amount of interparticle and intercrystalline porosity throughout. The amphipora-floatstone facies has vugular porosity caused by leaching of stromatoporoids. This interval is commonly fractured. Its bitumen saturation is lower than all other intervals. The upper Grosmont D subunit is a relatively clay-free, bitumen-saturated, laminated dolomite grainstone. The lower portion of this interval is commonly a brecciated dolomite indistinguishable from the lower Grosmont D breccia.

Fig. 2 shows the Grosmont C and D subunits. The Grosmont flow units comprise three permeability and porosity systems: (1) matrix, (2) vugs connected by crack, and (3) fractures. The core photos in Fig. 2 include examples for disaggregated dolomite from the lower D subunit with matrix and fracture porosity, and from the middle C subunit dominated by vug porosity.

The discussion in this paper distinguishes between matrix and fracture pore space. Vugs are generally considered part of the fracture pore space but merge into matrix pore space as the vug size becomes small. **Table 2** lists the total porosity and saturation.

TABLE 2—POROSITY AND SATURATION DISTRIBUTION IN GROSMONT SUBUNITS AS DEFINED IN FIG. 2

	Total Porosity	Fraction of Fracture and Vug Porosity	Oil Saturation
Upper D	0.25	0.10	0.82
Middle D	0.18	0.50	0.65
Lower D	0.30	0.10	0.80
C/D Marl	0.15	0.01	0.60
Upper C	0.16	0.50	0.75
Middle C	0.32	0.05	0.82
Small vugs	0.18	0.50	0.80
Large vugs	0.14	0.75	0.65
Volume Weighted Average			
Grosmont C	0.25	0.24	0.75
Grosmont D	0.18	0.52	0.75
Grosmont C + D	0.22	0.35	0.75

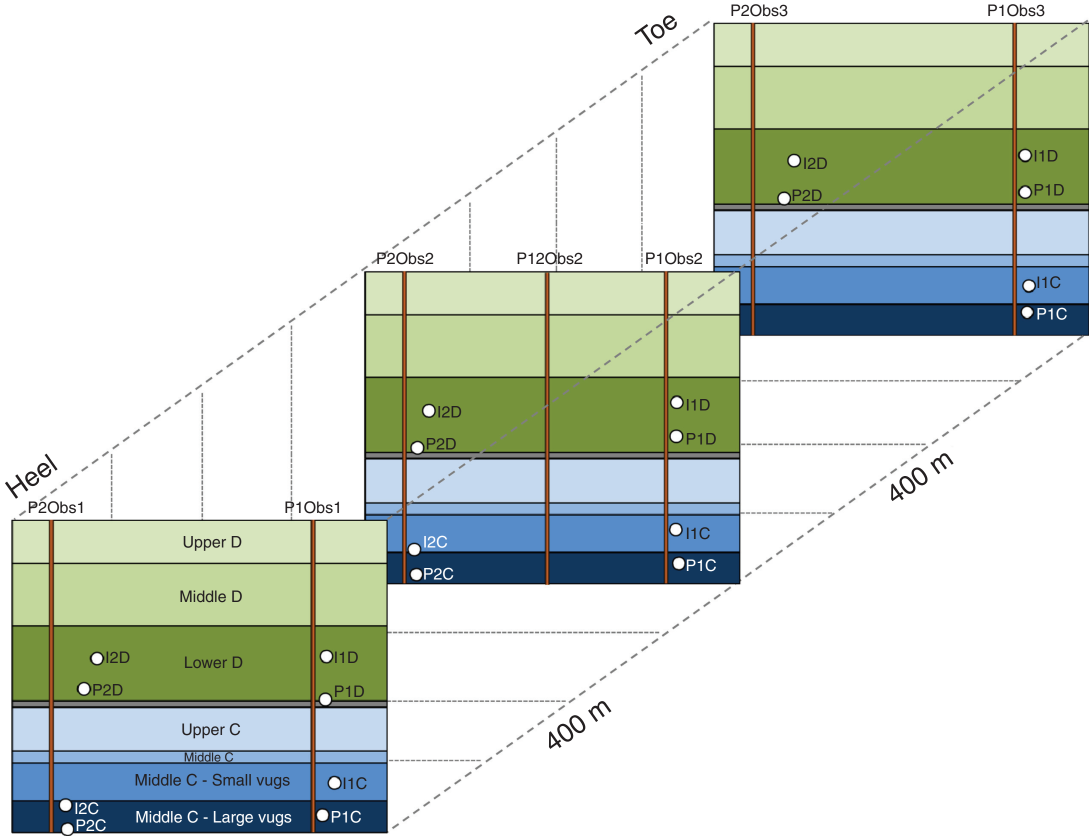

Fig. 3—Approximate well configuration.

The fraction of total pore space occupied by fractures and vugs is derived from computer-tomography scans of cores (Kantzas 1990). Matrix permeability is 150 to 250 md, and fracture permeability is > 10 darcies.

Drilling and Completion. A total of eight horizontal wells and seven vertical observation wells were drilled. Two SAGD well pairs are placed at the bottom of the Grosmont C unit and two at the bottom of the Grosmont D unit (Fig. 2). Lateral distance between the well pairs is 90 to 100 m, and the vertical offset between injector and producer is 4 to 6 m. Well Pairs 1C, 1D, and 2D are 800 m long, while Well Pair 2C is 450 m long. The location of the vertical observation wells is indicated in **Fig. 3,** and the lateral distances between horizontal and observation wells are listed in **Table 3.**

The horizontal wells are drilled in three sections: surface section to the Ireton formation (approximately 300-m true vertical depth (TVD) and 60 to 70° inclination) with casing to surface, intermediate section (350- and 370-m TVD for Grosmont D and C units, respectively, with 90° inclination) with casing, and lateral section (90° inclination).

TABLE 3—LATERAL DISTANCE OF OBSERVATION WELLS FROM HORIZONTAL WELLS (m)

	P1C	I1C	P1D	I1D
P1Obs1	4	10	6	6
P1Obs2	6	3	4	4
P1Obs3	6	7	5	5
	P2C	I2C	P2D	I2D
P2Obs1	8	7	16	22
P2Obs2	6	3	6	12
P2Obs3	N/A	N/A	15	19

Between February and March 2008, Well P2D was drilled completely, as well as the surface and intermediate section of I1C. The lateral section of I1C was completed in August 2010. Wells P1C, P1D, I1D, and I2D were drilled between January and March 2010. Wells P2C and I2C were added between January and March 2012.

The surface sections usually took 2 to 3 days to drill. Mud and cement losses in the intermediate section were significant, and these intervals needed more time (on average 12 days up to 44 days). The lateral section required on average 10 days. Total drilling time averaged 24 days for each horizontal well.

The 2C well pair was drilled at balanced conditions using a foam-circulating system; all of the previous wells were drilled overbalanced with water-based fluid. The casings for the surface section ($13\frac{3}{8}$ in.) and the intermediate section ($9\frac{5}{8}$ in.) are cemented to surface. Well Pairs 1C, 1D, and 2D have uncemented slotted liners in a $8\frac{3}{4}$ in. hole; Well Pair 2C is openhole in the lateral section. **Table 4** lists the details of completions, including pressure and temperature monitors.

All wells were treated with acid at different times and scales. During the campaigns, after 6 to 8 months of operations, approximately 30 m^3 of nitrified acid was injected to the heel and/or the toe of Well Pairs 1C and 1D, totalling 60 to 90 m^3 of acid for each well. Well Pair 2C and Well I2D were acidized before any operations, using eight stages for Well Pair 2C (each 50 m long) and three stages for Well I2D (each 265 m long). Total acid volumes were 160 m^3 for Well I2D and 180 m^3 for each 2C well. Normalized to the well length, the acid volumes are 0.1 m^3/m for 1C and 1D wells, 0.2 m^3/m for I2D, and 0.4 m^3/m for 2C wells.

Facilities. The Saleski pilot facilities were built initially for SAGD operations and completed in 2010. The plant has been upgraded since then. Currently, 840 t/d of steam can be generated at 10 mPa and 75% quality. After passing through a steam separator, 98% steam quality is delivered to the wellheads with a maximum pressure of 3.5 MPa. Treatment capacities are 800 m^3/d for

TABLE 4—WELL COMPLETIONS

	Slotted Liner	Tubing				Pressure			
		Heel		Toe		Bubble Tube	Fibre		Temp.
							Heel	Toe	Fibre
Size (in.)	7	$3^1/_2$	$4^1/_2$	$2^3/_8$	$3^1/_2$	–	–	–	–
P1C	X		X	X		init.	X		X
I1C	X	X			init.				
P1D	X		X	X		X			X
I1D	X	X			init.				
P2C			X	X			X	X	X
I2C		X			X				
P2D	X				X			X	X
I2D	X		X	X			X	X	

init. = indicates the initial completion with a subsequent change.

water, 290 m^3/d (1,800 B/D) for bitumen, and 3,000 std m^3/d for gas. Diluent is added to the produced bitumen (forming "DilBit") to meet sales specifications for density, viscosity, and water content. Diluent and DilBit are transported to and from the facilities by trucks. The infrastructure is coordinated with Laricina's Germain SAGD surface facilities (targeting the upper Grand Rapids formation) in close proximity to the west of Saleski.

Overview of Operations. Fig. 4 shows an overview of the Saleski well operations. The initial Wells P1C, I1C, P1D, and I1D were operated with continuous injection and production for the first year. Both producer and injector wells were warmed up by steam injection (bullheading). During the subsequent operations, continuous steam injection into the injectors and continuous production from the producers were occasionally interrupted by the need for workovers. In addition, producers had to be warmed up by steam injection for flow assurance.

After a successful test in P1C in early 2012, the decision was made to operate cyclic steam injection and production from individual Wells P1C, P1D, P2C, and I2D. The addition of P2C and I2C in March 2012 provided the opportunity to start a new well in a cyclic fashion. The performance of the cyclic operations improved with respect to SOR and CDOR compared with continuous production and injection. This change in operational strategy created new challenges for the facility that was built for SAGD operations. Occasionally, short tests of continuous production and injection were conducted by injecting into the injector and producing simultaneously from the producer (I1D and P1D in January 2013; I2C and P2C in June 2013).

A useful analytical plot for thermal processes is recovery factor (RF) as a function of pore volume of steam injected (see **Table 5** and Appendix A for details). **Fig. 5** illustrates the maturity of the pilot: The steam injected per well pair is less than 60% of the drainage box pore volume (PV), and less than 10% of the bitumen has been recovered per pair. Relative to the larger PV and net pay in the Grosmont D unit (Table 2), the current volumes injected and produced in this unit are small compared with the impacted PV in the Grosmont C unit. Therefore, the following discussion of the Saleski pilot is limited to the performance of Well Pairs 1C and 2C in the Grosmont C units.

Pilot Performance in Grosmont C Unit

Continuous Period. The continuous-injection-and-production period in the Grosmont C reservoir covers April 2011 to mid-January 2012. **Fig. 6** shows injection and production rates together with pressure and temperature data for Well Pair 1C. Observation-well-temperature data show no significant trends, and are not discussed here.

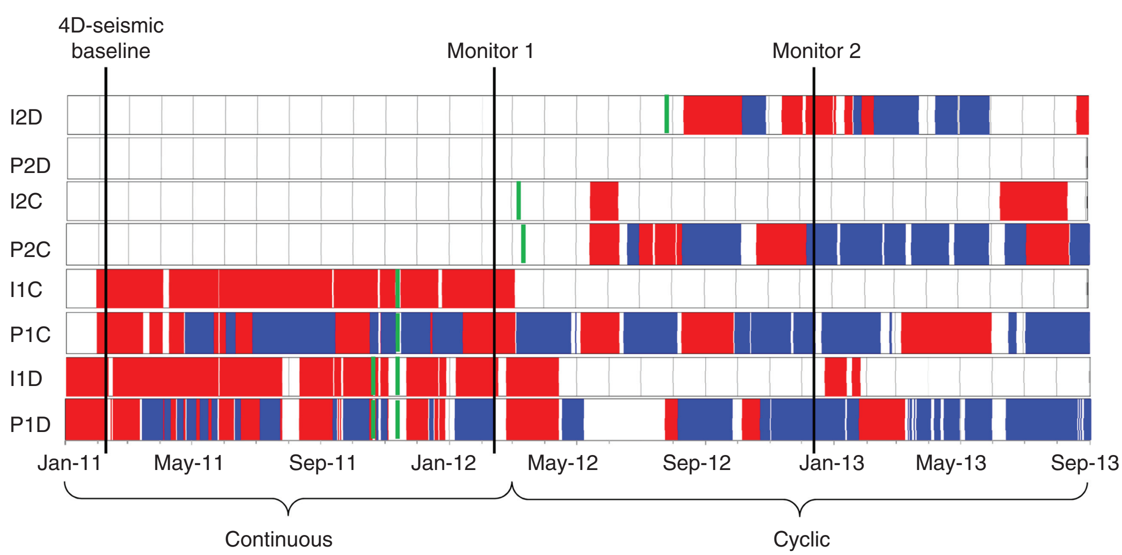

Fig. 4—Overview of Saleski well operations. Vertical axis: well name (see Fig. 2); red = steam injection; blue = production; white = idle; and green = acid treatment. Vertical black lines indicate dates of time-lapse-seismic acquisition.

TABLE 5—PARAMETERS USED TO CALCULATE PV AND RF*

	Well Length (m)	Well Spacing (m)	Pay Above Producer (m)	Porosity	PV (10^3 m^3)	S_o**	*OBIP*† (10^3 m^3)
1C	800	100	18	0.18	292	0.75	219
1D	800	100	28	0.25	630	0.79	498
2C	450	100	20	0.18	198	0.75	149
2D	800	100	22	0.25	495	0.79	391

* see Appendix A for details.
** S_o = initial oil saturation.
† *OBIP* = original bitumen in place.

Between the end of June and mid-September 2011, a stable period of continuous-production-and-injection operations was achieved for 78 days. The calendar-day steam rate at the end of this period was 210 t/d, with a total volume of 16 500 t injected. With 2200 m^3 of bitumen produced, the SOR is 7.5 and the CDOR is 28 m^3/d at the end of the period. These metrics are challenging for economic development.

For the first part of this period, steam was injected at 210 to 220 t/d, and then raised to 230 to 240 t/d to address the low CDOR. However, average oil rates decreased from 32 to 25 m^3/d, and average water rates from 170 to 135 m^3/d. The increased steam rate resulted neither in higher oil rates nor in a water breakthrough. Temperature data along the producer indicate that the higher steam rate developed an improved connection at the toe, which remains evident in all subsequent operations.

During the period of stable gravity-drainage operations, the bottomhole-pressure (BHP) difference between producer and injector is 1500 to 2000 kPa (Fig. 6), compared with an expected 50-kPa head difference for the 5 m offset. Bottomhole temperature (BHT) in the producer is between 120 to 150°C, sufficient to reduce the bitumen viscosity to 100 to 500 cp.

Between October 2011 and January 2012, the 1C well pair was treated with acid during continuous-injection-and-production operations. The large pressure difference between injector and producer was reduced, and initial oil rates increased (Fig. 6). However, these rates could not be maintained. During November 2011, the emulsion and oil rate being produced from P1C was observed to increase after steam injection into I1C was shut off. This led to the testing of a production period without any steam injection, from mid-November to mid-December. The results from this cycle were then compared with the continuous-injection-and-production cycles that had occurred up to that point, where P1C produced less than 50 m^3/d of bitumen compared with approximately 80 m^3/d of bitumen under the cyclic operation.

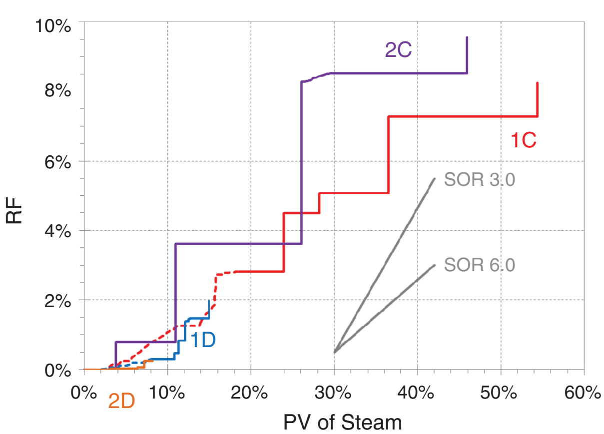

Fig. 5—RF as a function of PV_{inj} (see Appendix A for details) for each well pair. Dashed lines = continuous period, solid lines = cyclic period, grey lines = example slopes of SOR values of 3.0

To verify this interpretation, a continuous-injection-and-production test was conducted with Well Pair 2C in mid-June 2013 after a cyclic operation of P2C for 1 year. The test demonstrated that it is possible to balance injection and production volumes, and to achieve a low subcool, while the pressure difference between injector and producer is hydrostatic (40 to 70 kPa). These are all indicators for successful conventional SAGD operation.

The test also demonstrated the impact of borehole hydraulics. The steam-injection rate was split evenly between short and long tubing (for completions, see Table 4), which creates a pressure difference of 200 kPa between the heel and the toe of the wellbore. This pressure gradient exceeds the gravitational force between injector and producer, thereby interfering with the SAGD process (e.g., Edmunds and Gittins 1993).

The attempt to achieve SOR and CDOR values that are comparable with conventional SAGD by operating the Saleski pilot well pairs with continuous injection and production was influenced by constraints of the pilot plant and artificial lift, and by potential well impairment. The results of the first pilot period are not sufficient to exclude SAGD as a viable recovery mechanism in the Grosmont formation. Cyclic operation is less sensitive to the previously mentioned constraints.

Cyclic Period. With the transition to a cyclic process at the end of 2011, it was apparent that additional steam capacity was required in order to sustain production from the pilot. Through 2011, it was also noted that the individual wells demanded more steam than was available from one once-through steam generator (OTSG). An additional 50-million-Btu/hr OTSG was added to the facility in December 2011. This increased the steam capacity from 425 t/d to approximately 850 t/d. The additional steam capacity provides the flexibility to operate more than one well or well pair.

In addition to the OTSG, it was decided to add another well pair to the pilot. The recommendation was completed before the cyclic testing that occurred at the end of 2011. As described previously, steam capacity was a key consideration and consequently the wells were planned to be shorter (450-m horizontal sections).

In cyclic operation, steam is injected through one well, and bitumen and condensed steam are produced back through the same well. For the Grosmont C unit, Wells P1C and P2C were chosen for cyclic operations. The cyclic period shown in **Figs. 7 and 8** started mid-January 2012, continued at the time of writing for P1C, and covered May 2012 to mid-June 2013 for P2C; after mid-June 2013, the continuous-injection-and-production test discussed previously was executed.

Comparing the performance of cyclic operations for wells in the Grosmont C unit (Table 4), the following aspects have to be considered:

- 1C wells have a horizontal section that is 800 m long; 2C wells have a horizontal section that is 450 m long.
- 1C wells were drilled overbalanced; 2C wells were drilled at balanced conditions.
- 1C wells are completed with a slotted liner; 2C wells are completed open hole.
- 1C wells were acidized at the heel and toe through tubing (acid wash) after 6 to 8 months of operations; 2C wells were

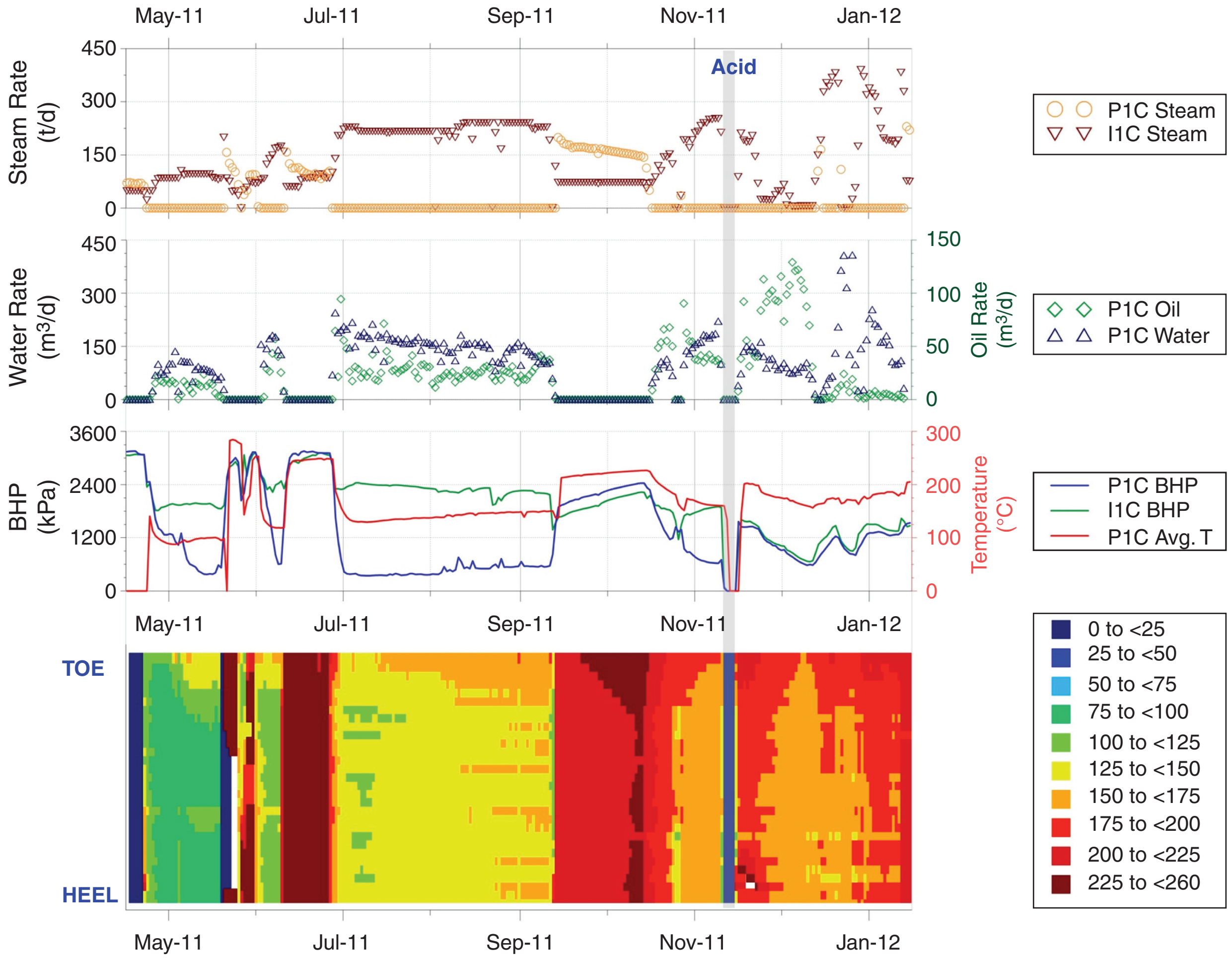

Fig. 6—Well Pair 1C data for continuous-injection-and-production period April 2011 to February 2012. Top: steam-injection rates; second from top: water- and bitumen-production rates; third from top: BHP and BHT; and bottom: flowing temperature profile in °C along producer.

acidized in 50-m stages using openhole packers before steaming (acid stimulation) immediately after completions.

In terms of CDOR and SOR, cyclic performance exceeds continuous-injection-and-production performance, and P2C outperforms P1C. It is remarkable that the CDOR of a 450-m-long horizontal well (P2C) is higher than that of an 800-m-long well (P1C).

Fig. 9 shows the temperature data collected in the observation wells (see also Fig. 3 and Table 3). P2Obs1 was damaged during installation, and is not considered in the discussion. Significant temperature response during periods of steam injection is observed in the Grosmont C unit. Temperature increase in the Grosmont D unit is minor and continuous, indicating conductive heating. At the observation wells, the hot region is limited vertically to the middle C subunit (Fig. 2). A recent temperature increase in the upper C subunit at P2Obs2 and P12Obs2 is related to the most recent (August 2013) injection cycle in the 2C well pair; this cycle is not discussed here because of the lack of production data.

Injectivity. Fig. 10 compares the downhole pressure (measured by a gauge close to the pump intake) during injection for each cycle of P1C with that of P2C. Steam-injection rates and cumulative steam volume per cycle are normalized to a 1-m-well length to accommodate for the different lengths of P1C (800 m) and P2C (450 m). For P1C, injectivity improved significantly from Cycles 1 to 2; at higher rates, injection pressure is lower. Cycles 3 and 4 show similar injection pressure, despite higher rates and volumes in Cycle 4.

During the first cycle in P2C, pressure data were not available. The second cycle of injection has the characteristics of the removal of a plug in the wellbore region. The injectivity decreases toward 15 m^3 cumulative steam per metre of well injected, and then suddenly increases (pressure declines, rates increase). The following cycle shows lower injection pressure at higher injection rates, indicating a successful removal. Cycle 4 was operated at injection rates comparable with those of the second cycle, and shows lower injection pressure. Cycles 3 and 4 also show a backpressure from the reservoir that increases with cumulative volume. In terms of CDOR and SOR, cyclic performance exceeds continuous injection and production performance, and P2C outperforms P1C **(Table 6).**

Comparing Cycle 4 of P1C with Cycle 3 of P2C, the maximum injection pressure is higher in P1C although injection volumes are comparable with (on a per metre well basis), and injection rates are larger for, P2C. The injection pressure difference of 600 kPa (2100 and 2700 kPa for P2C and P1C, respectively) translates into a 15°C difference of injected-steam temperature (215 and 230°C for P2C and P1C, respectively).

In-situ stress tests above the Grosmont D unit showed that the minimum-stress orientation is vertical (i.e., in order to fracture the rock, the pore pressure has to exceed the overburden stress). In the Grosmont formation, the rock is already fractured. On the basis of density logs in the overburden, the pore pressure required to lift the overburden is 6800 to 7900 kPa for the depth interval between top Grosmont D unit and bottom Grosmont C unit (325 and 375 m, respectively). Injection pressures observed at the pilot are less than 40% of this critical pore pressure.

3D-seismic surveys were shot in February 2011 (baseline), February 2012 (Monitor 1), and December 2012 (Monitor 2), as indicated in Fig. 4. **Fig. 11** shows the impedance (product of density and seismic velocity) difference of Monitor 2 to the baseline, together with the operational status of the horizontal wells at the

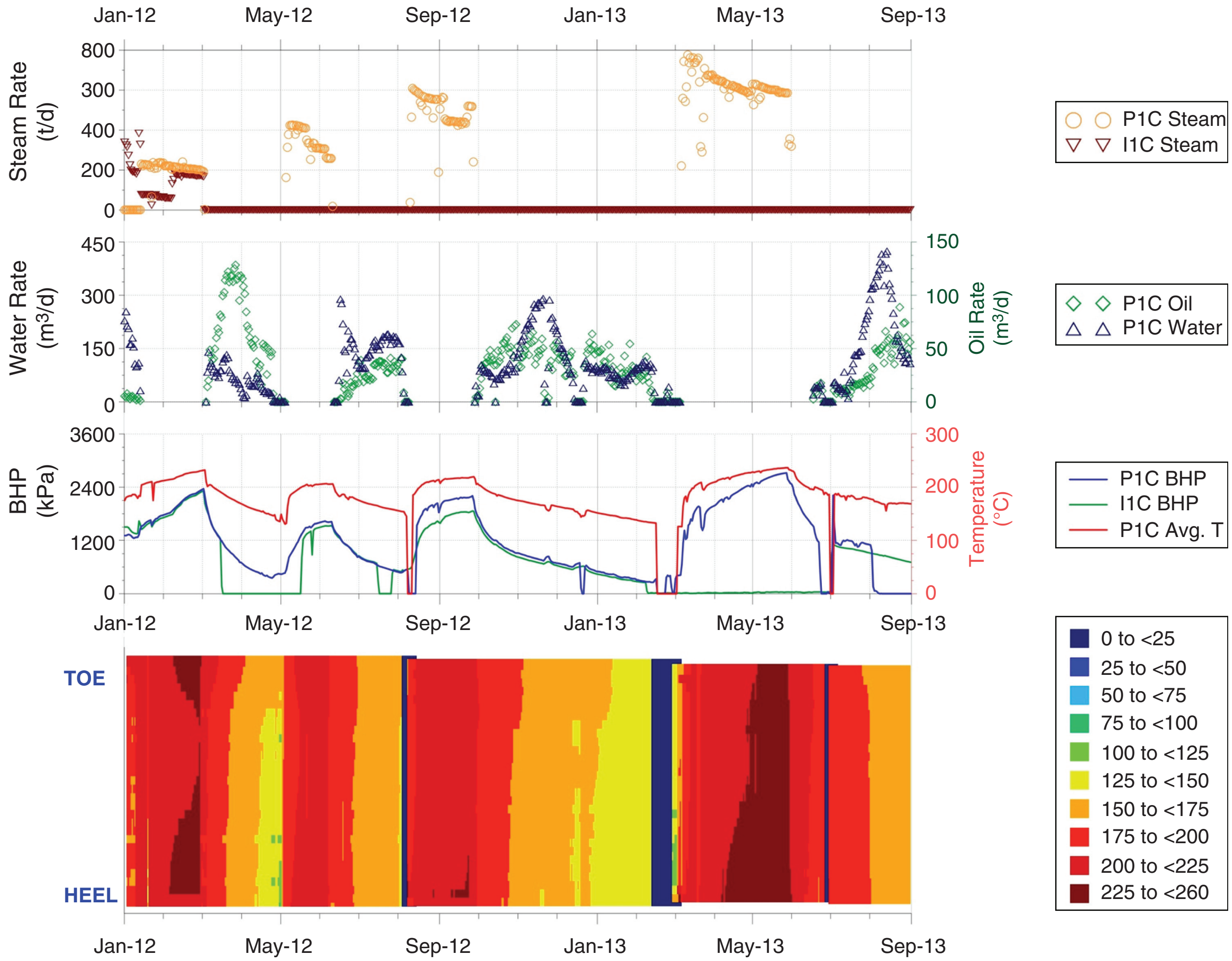

Fig. 7—Well Pair 1C data for cyclic period, January 2012 to September 2013. Top: steam-injection rates; second from top: water- and bitumen-production rates; third from top: BHP and BHT; and bottom: flowing temperature profile in °C along producer.

time Monitor 2 was shot. Pressures at that time range from 650 (P1Obs2) to 1000 kPa (P2Obs2). The blue area indicates areas in the reservoir where seismic impedance has been impacted by the pilot operations. Conformance along the wells is close to 100%. The impacted volume is contained around the wells. First connections between 2C and 1C wells are developing.

Productivity. The decline of production rates during a cycle is commonly a function of reservoir-pressure reduction. In the fractured carbonate, reservoir pressure is not the main drive mechanism and the oil-rate decline is more a function of BHT (**Fig. 12**). This is related to the sensitivity of bitumen viscosity to temperature (Yang et al. 2014). During the pilot operations, cycle performances have been forecasted successfully by applying a decline-curve analysis on the basis of BHT reduction.

Although P2C has only 55% of the P1C well length available, absolute oil rates exceed P1C production. The production interval of P1C is 130 to 180°C, while P2C performs between 80 and 165°C. The ability of P2C to produce more-viscous bitumen is an indicator that P2C has a better productivity index, or that P1C is affected by skin. This is aligned with the balanced drilling, openhole completion, and staged acid stimulation of P2C, compared with overbalanced drilling, slotted-liner completion, and acid wash for P1C.

P1C production starts at temperatures approximately 15 to 20°C higher because of the higher injection pressure required during steam injection (see previous discussion of injectivity). Upon production, BHP declines and water in the well flashes into steam. **Fig. 13** shows BHT and BHP during production in comparison to steam. While P2C operates in the liquid area of the phase diagram, P1C bottomhole conditions are close to or in the vapour phase. Any gas phase reduces the efficiency of the progressing cavity pumps used to lift the fluids.

Fig. 14 compares the oil rates and BHP of P1C with P2C as a function of cycle ratio of produced fluid volume to total steam volume injected [total fluid/steam ratio (TFSR)] for an individual cycle. Despite almost twice the well length, P1C oil rates are on a lower level than P2C rates, indicating a lower productivity index for P1C. In Cycles 1 and 2 of P2C, the initial peak production reaches 200 m^3/d; Cycle 3 potentially has the same behaviour but is interrupted by a pump change. The initial peak rate of P1C is observed only in the first cycle.

Cycles 2 and 3 in P1C and Cycle 2 in P2C show indications for 40- to 60-m^3/d plateau rates; however, the data illustrate the difficulty to maintain a plateau production with pilot operations. For both wells, production periods had to be cut short because of steam-schedule issues. To maintain the facility heat integration, steam injection has to continue during production. Some P1C production cycles were experiencing lift problems because of water flashing in the well (see previous discussion).

Cycle 3 in P2C clearly indicates well communication to P1C (90- to 100-m lateral distance). The start of steam injection into P1C increases BHP in P2C and reduces the bitumen rate (while water cut increases). During a 5-day shut-in of P2C for a pump repair, BHP increases rapidly because of pressure support from P1C. The subsequent BHP during production is stable but at a high level. At TFSR = 1.2 in Cycle 3, the water depletion index

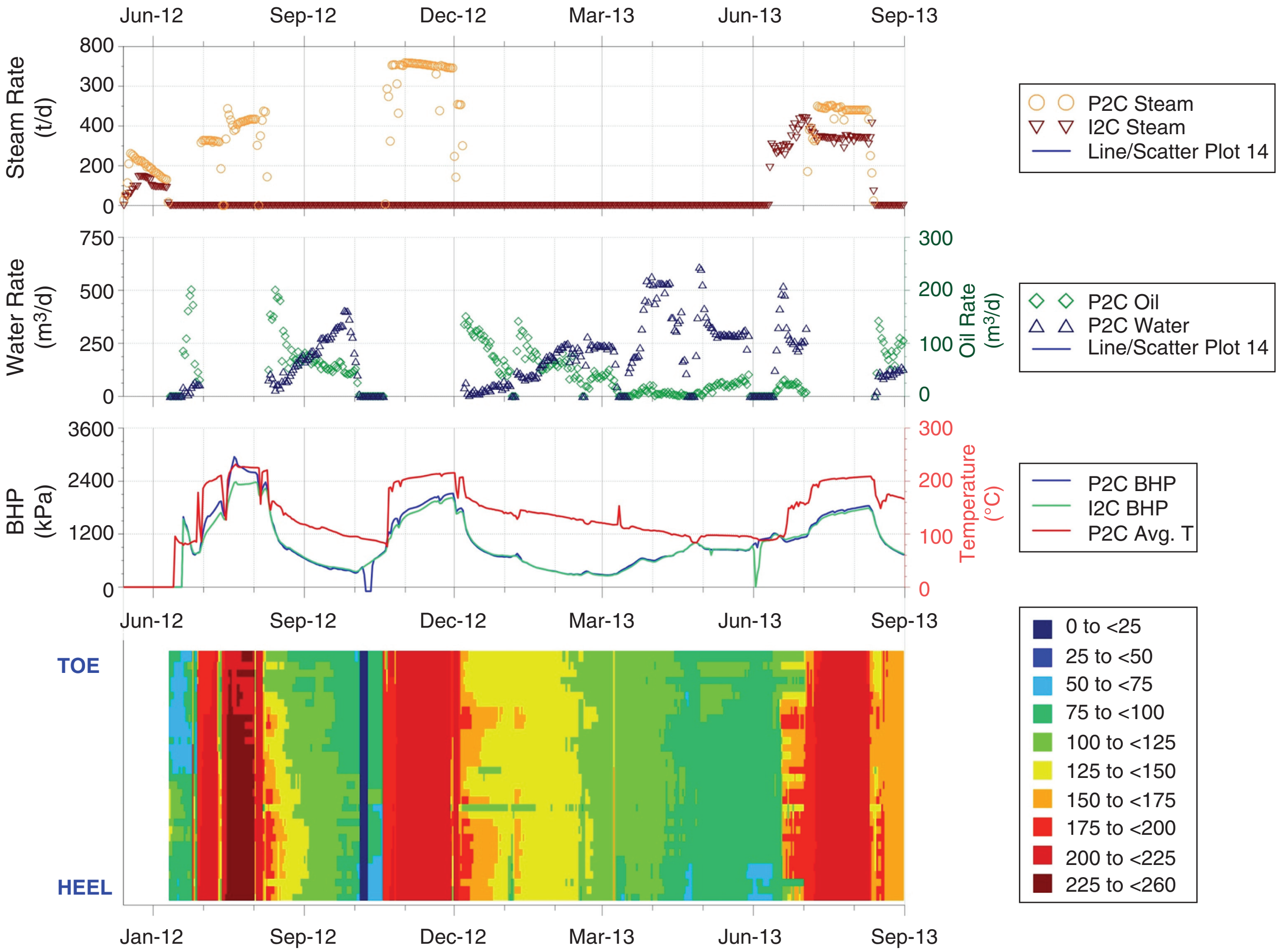

Fig. 8—Well Pair 2C data for cyclic period, May 2012 to September 2013. Top: steam-injection rates; second from top: water- and bitumen-production rates; third from top: BHP and BHT; bottom: flowing temperature profile in °C along producer.

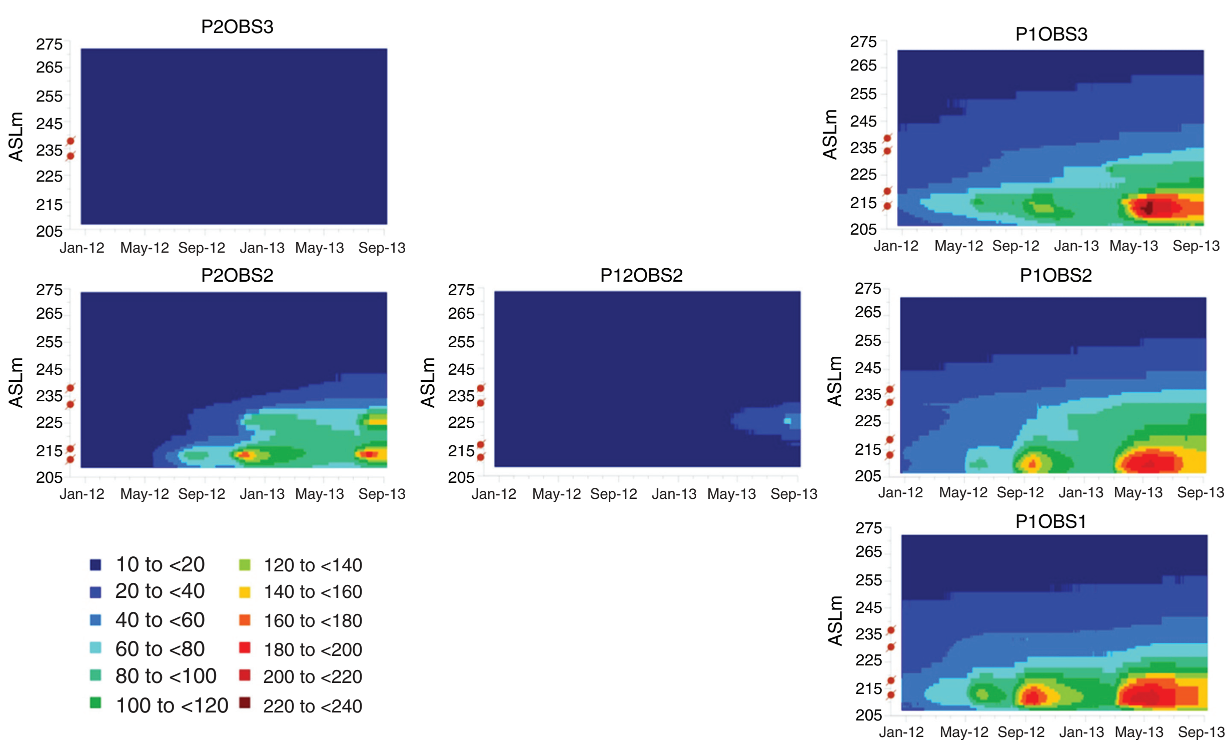

Fig. 9—Observation-well temperature data in °C. Red circles indicate vertical location of horizontal wells. For lateral distance between observation well and horizontal well, see Table 2; for general well locations see Fig. 3.

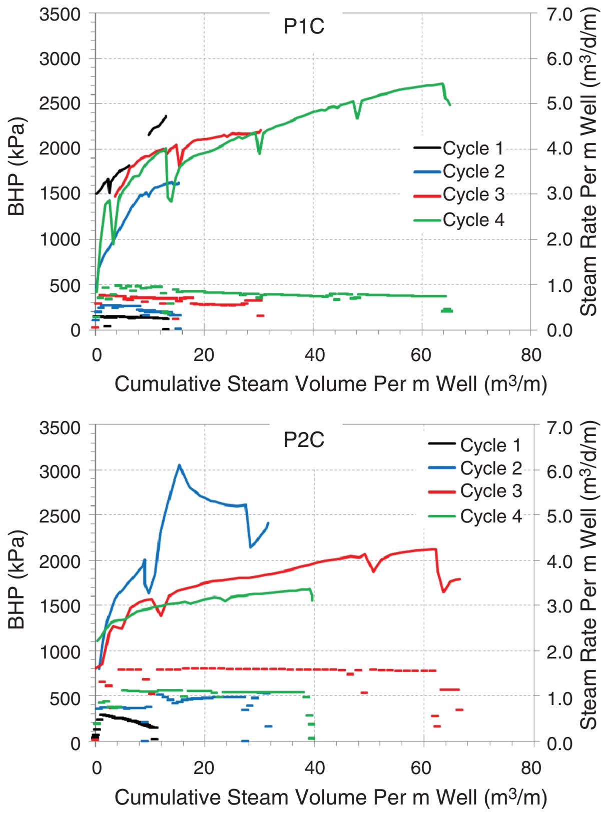

Fig. 10—Per cycle, BHP as function of cumulative injected steam volume per metre of well length (solid lines), together with injection rates per metre of well length (horizontal bar symbols). Top: P1C; bottom: P2C. BHP data are not available for P2C Cycle 1.

reaches a value of 1.0 (i.e., the total cycle's steam injected is produced as water). Subsequently, pressure support from P1C steam injection maintains fluid production at high BHP, while the bitumen rate increases because all injected water is already produced.

The developing well interference is supported by 4D seismic (Fig. 11). In principle, well communication can be turned into an advantage by operating the wells synchronically. However, the limited pilot-plant capacity for steam generation prevents simultaneous injection into P1C and P2C at the desired high rates.

The comparison of P1C and P2C shows higher injection pressure (Fig. 10), higher required BHT during production (Figs. 12 and 13), and lower bitumen rates (Fig. 14) for P1C, although the horizontal well section is almost twice that of P2C. This indicates a potential impairment of P1C, which can be related to the drilling conditions, the completion design, and/or the acid-treatment strategy. P2C performance is considered to be a closer representation of unimpaired reservoir behaviour, and therefore forms the basis for future depletion plans from the Grosmont formation.

Conclusions

The Saleski pilot, operated since December 2010, leads to the following conclusions:

- Steam injectivity into the bitumen-saturated Grosmont reservoir is high, even under initially cold reservoir conditions. Injection pressure remains less than 40% of the pore pressure required to lift the overburden.
- Steam conformance along the injection well is close to 100%.
- Heat is confined to the nearby region of the injection well.
- The attempt to achieve SOR and CDOR values that are comparable to those of conventional SAGD by operating the Saleski plot well pairs with continuous injection and production was influenced by constraints of the pilot plant and artificial lift, and concern for potential well impairment.

TABLE 6—PERFORMANCE OF GROSMONT C PILOT WELLS

		CDOR (m^3/d)	SOR
P1C/I1C			
Continuous	Apr 2011–Jan 2012	23	5.4
P1C			
Cycle 1	Jan 2012–Apr 2012	36	4.4
Cycle 2	May 2012–Aug 2012	14	9.6
Cycle 3	Aug 2012–Mar 2013	24	5.0
Cycle 4*	Mar 2013–ongoing	–	–
	31 Aug 2013 data	12	26
	End-of-cycle estimate	25–30	4.2–4.7
P2C/I2C			
Continuous	Jun 2013–Jul 2013	16	21
P2C			
Cycle 1/warm-up	May 2012–Jun 2012	25	6.5
Cycle 2	Jun 2012–Oct 2012	43	3.4
Cycle 3	Oct 2012–May 2013	31	4.3
Cycle 4*	Jul 2013–ongoing	–	–
	31 Aug 2013 data	26	26
	End-of-cycle estimate	45–55	3.7–4.5

* Note: Values for Cycle 4 are not final.

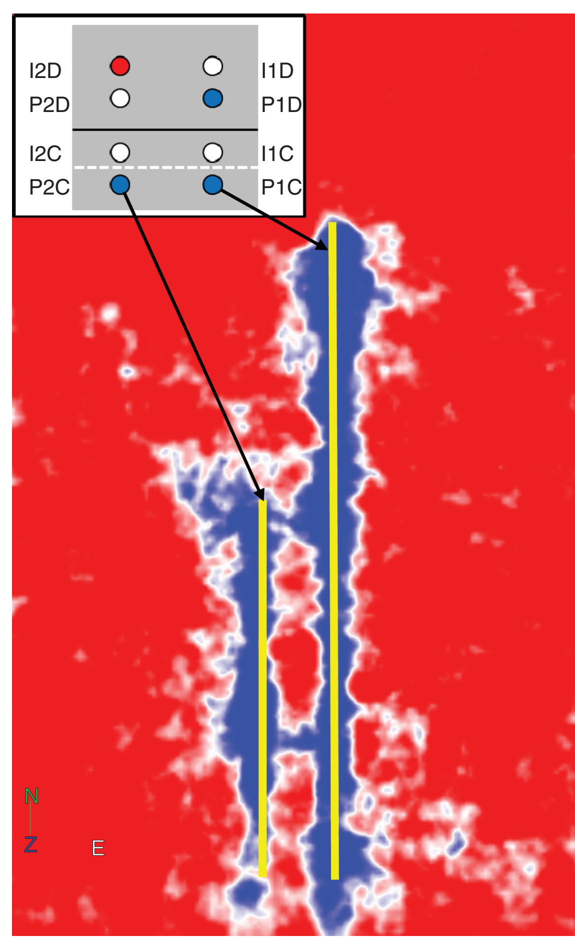

Fig. 11—Plan view of 3D-seismic impedance difference (from prestack inversions) between Monitor 2 (December 2012) and baseline (February 2011). Differences increase from red (zero) to blue [–0.7 kg/(m^2 s)]; yellow lines indicate horizontal wells in Grosmont C; the inlet shows a cross section with approximate location of the slice (white dashed line) and horizontal wells (circles); at the time Monitor 2 was shot, wells were idle (white), on production (blue) or on injection (red).

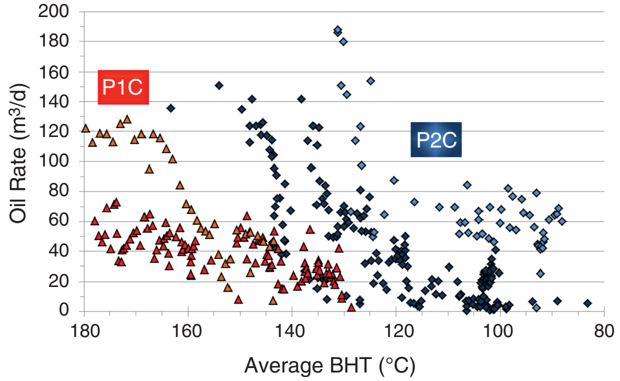

Fig. 12—Decline of oil rate as a function of BHT for two cycles (lighter and darker colour) from P1C (triangles) and P2C (diamonds). The horizontal axis is reversed because the well cools down during production.

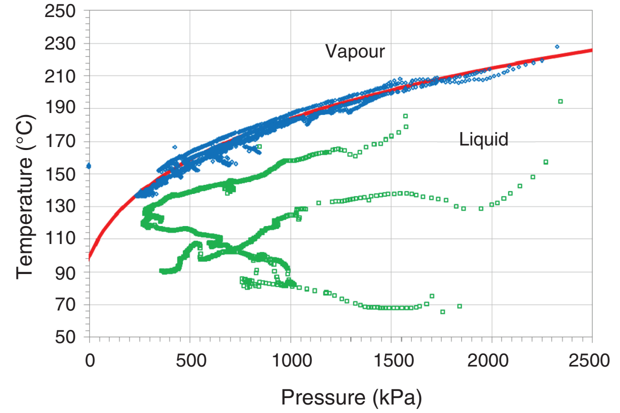

Fig. 13—Phase diagram of steam (red line) and bottomhole conditions during production (first three cycles) for P1C (blue symbols) and P2C (green symbols).

- The results of the first pilot period are not sufficient to exclude SAGD as a viable recovery mechanism in the Grosmont formation.
- Cyclic operation of individual wells has the potential to improve the performance indicators over continuous-injection-and-production operations, but it creates lift challenges in wells operated close to steam-saturation conditions.
- P1C is potentially impaired, which can be related to the drilling conditions, completion design, and/or the acid-treatment strategy; P2C behaviour is more representative of reservoir performance, and is considered as the base case for planning.
- A cycle CDOR of 43 m^3/d (270 B/D) for a 450-m-long well was achieved with an SOR of 3.4 in P2C.

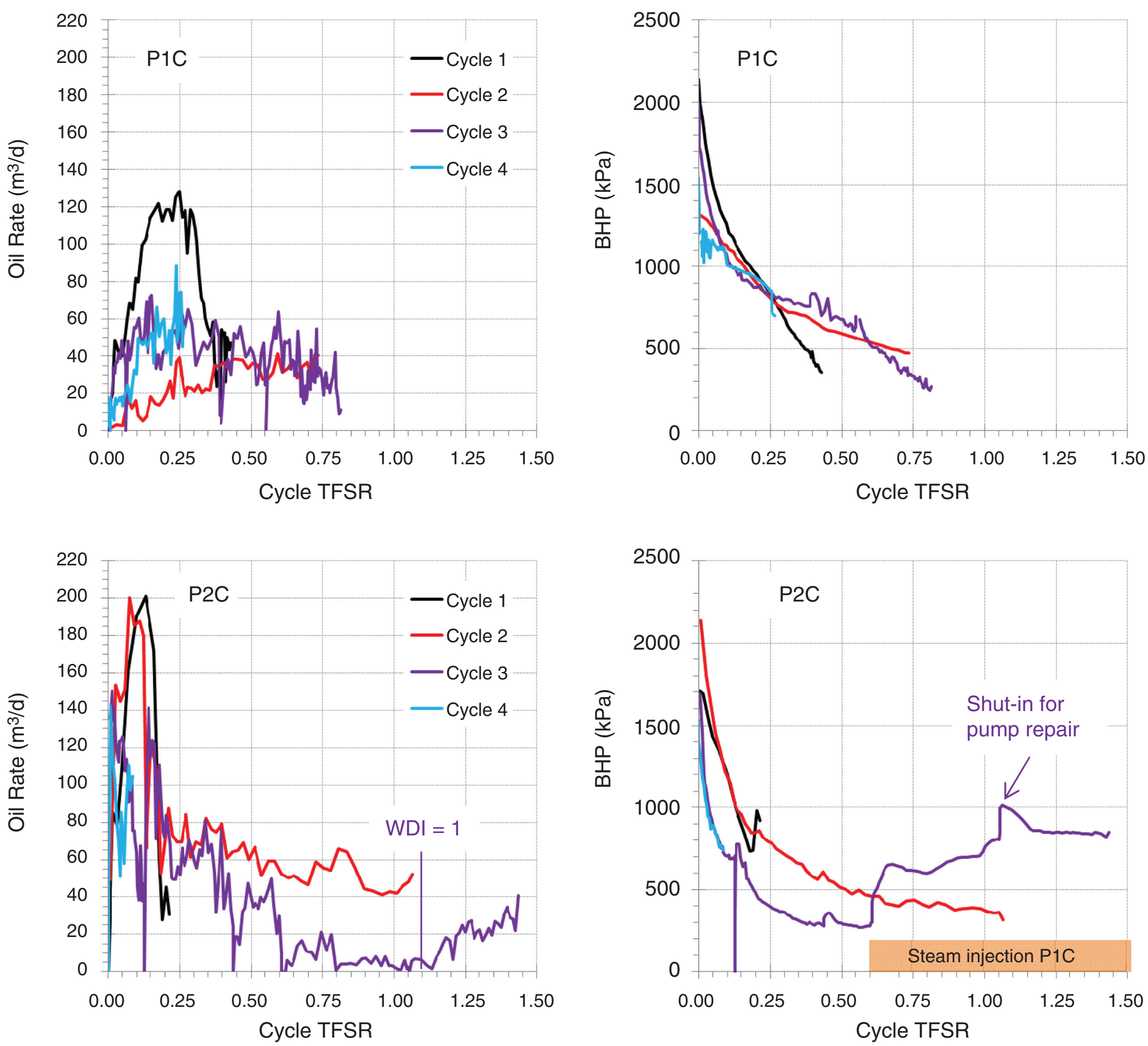

Fig. 14—Comparison of oil rates (left) and BHP (right) for P1C (top) and P2C (bottom) as a function of cycle TFSR.

- The reservoir performance of the Saleski Grosmont C unit is derisked; optimization of well placement, drilling conditions, well completions, and lift systems will improve the performance of commercial projects.

Acknowledgements

The authors thank Laricina Energy Limited and Osum Oil Sands Corporation for permission to publish this paper. We also thank numerous team members from both companies for contributing to the discussions, and internal reviewers for their comments.

References

Burrowes, A., Teare, M., Marsh, R. et al. 2011. Alberta's Energy Reserves 2011 and Supply/Demand Outlook 2012-2021. Annual Report ST98-2011, Energy Resources Conservation Board, Calgary, Alberta (June 2011).

Barrett, K.R. and Hopkins, J.C. 2010. Review of Geology of a Giant Carbonate Bitumen Reservoir, Grosmont Formation, Saleski, Alberta. In Heavy Oils: Reservoir Characterization and Production Monitoring, ed. S. Chopra, L.R. Lines, D.R. Schmitt, and M.L. Batzle, No. 13, Section 2, Chap. 10, 155-163. Tulsa, Oklahoma: Geophysical Developments Series, Society of Exploration Geophysicists.

Edmunds, N. and Gittins, S.D. 1993. Effective Application of Steam Assisted Gravity Drainage of Bitumen to Long Horizontal Well Pairs. *J Can Pet Technol* **32** (6). PETSOC-93-06-05. http://dx.doi.org/10.2118/93-06-05.

Husky Oil Operations. 2013. Saleski Thermal Experimental Project, Application for Approval (1761641), submitted to Alberta Energy Regulator 2013.

Kantzas, A. 1990. Investigation of Physical Properties of Porous Rocks and Fluid Flow Phenomena in Porous Media Using Computer Assisted Tomography. *In Situ* **14** (1): 77–132.

McDougall, J., Alvarez, J.M., and Isaacs, E. 2008. Alberta Carbonates - the Third Trillion. Presented at the 19th World Petroleum Congress, Madrid, Spain, 29 June–3 July. WPC-19-0925.

Solanki, S.C., Barrett, K., Riva, D. et al. 2011. The first SC-SAGD Pilot in the Grosmont. Presented at the 2011 World Heavy Oil Congress, Edmonton, Alberta, Canada, 14-17 March. Paper No. WHOC11-615.

Yang, D., Hosseininejad Mohebati, M., Brand, S. et al. 2014. Thermal Recovery of Bitumen from the Grosmont Carbonate Formation - Part 2: Pilot Interpretation and Development Strategy. *J Can Pet Technol* **53** (4): Special Issue. SPE-171561-PA. http://dx.doi.org/10.2118/171561-PA.

Yuan, J.-Y., Jiang, Q., Russel-Houston, J. et al. 2010. Evolving Recovery Technologies Directed Towards Commercial Development of the Grosmont Carbonate Reservoirs. Presented at the Canadian Unconventional Resources and International Petroleum Conference, Calgary, 19–21 October. SPE-137941-MS. http://dx.doi.org/10.2118/137941-MS.

Appendix A—PV Injected vs. RF

A useful analytical plot is RF as a function of PV of steam injection. PV is defined as **(Fig. A-1)**

$$PV = L \cdot W \cdot H \cdot \phi, \quad \text{(A-1)}$$

with L as the well drainage box length, W the well drainage box width, H the well drainage box height, and ϕ the porosity.

The length of the drainage box is the well length, so half the distance to the next well at both ends of the well; the drainage box width is the distance to the next well; and the drainage box height is the net pay above the producer.

The original bitumen in place (OBIP) is calculated with

$$OBIP = PV \cdot S_O, \quad \text{(A-2)}$$

with S_O being the initial oil saturation.

The PV injected (PV_{inj}) is then calculated with

$$PV_{\text{inj}} = \frac{V_{\text{stm}}}{PV}, \quad \text{(A-3)}$$

with V_{stm} being the total volume of steam injected.

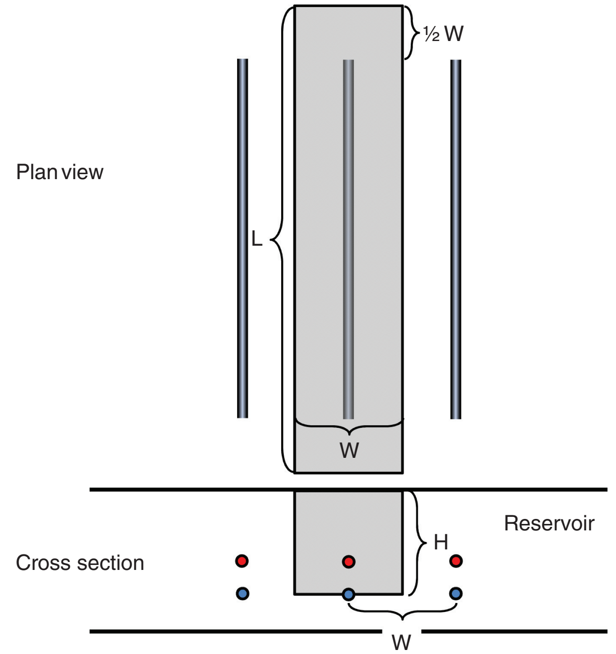

Fig. A-1—Well geometry for pore volume calculation.

The *RF* is

$$RF = \frac{N_p}{OBIP} = \frac{N_p}{PV \cdot S_O}, \quad \text{(A-4)}$$

with N_p being the total volume of oil produced.

In a plot of RF as a function of PV_{inj}, the slope is

$$\text{slope} = \frac{N_p}{PV \cdot S_O} \Bigg/ \frac{V_{\text{stm}}}{PV} = \frac{N_p}{S_O \cdot V_{\text{stm}}} = \frac{1}{S_O \cdot SOR}. \quad \text{(A-5)}$$

Moslem Hosseininejad Mohebati is a reservoir engineer currently with Laricina Energy Limited. Within Laricina, he is involved in design and optimization of production strategies for the Saleski pilot operation and supports the project Asset teams for Grosmont development. Hosseininejad Mohebati's primary areas of interest include steam- and solvent-assisted processes, in-situ recovery techniques and mechanisms for bitumen-bearing carbonate reservoirs, and design and scaling of experimental modelling of thermal processes. He has authored several technical papers in various journals and conferences. Hosseininejad Mohebati holds a PhD degree in petroleum engineering from the University of Calgary, and is a member of SPE and the Canadian Heavy Oil Association (CHOA).

Daniel Yang is Chief of Reservoir Engineering at Laricina. He dedicated 15 years of his oil-industry career to enhanced-oil-recovery methods, focussing on thermal recovery, and originating from 10 years of research in geothermal energy. Previously, Yang worked for Shell International, Shell Canada, and Canadian Natural Recourses. He graduated in Geophysics and has a PhD in Natural Sciences from the Technical University Berlin, Germany. Yang holds one patent, has authored several publications, and is member of SPE, the Association of Professional Engineers and Geoscientists of Alberta (APEGA), and CHOA.

Jeff MacDonald is a senior reservoir engineer at TransGlobe Energy Corporation and has more than 10 years of petroleum experience with Osum Oil Sands, Shell Canada, and ExxonMobil. He has covered a variety of assets, ranging from onshore/offshore conventional and unconventional gas plays to waterflooding, along with 6 years in heavy oil, including cold and thermal recovery of bitumen in clastic and carbonate reservoirs. MacDonald holds a BEng degree in chemical engineering from Dalhousie University. He is a member of SPE and APEGA.